Food Control 147 (2023) 109623

Contents lists available at ScienceDirect

Food Control

journal homepage: www.elsevier.com/locate/foodcont

Biomimetic magnetic nanoparticles for bacterial magnetic concentration in liquids and qPCR-detection

Monica Jimenez-Carretero, Javier Rodríguez-López, Cristina Ropero-Moreno, Juan Granada, Josemaría Delgado-Martín, Manuel Martinez-Bueno **, Antonia Fernandez-Vivas ***, Concepcion Jimenez-Lopez *

Department of Microbiology, University of Granada, 18071 Granada, Spain

ARTICLE INFO

Keywords:
Magnetic nanoparticles
MamC
Biosensor

ABSTRACT

The development of improved systems for the fast detection of trace amounts of infectious agents is of vital importance. Magnetic nanoparticles (MNPs) are an interesting alternative in this context due to (1) their large surface area, that maximizes the potential interaction between the target microorganism and the nanoparticle, and (2) their magnetic susceptibility, that allows the concentration of the nanoparticles (and thus, the attached microorganisms) by means of an external magnetic field. In the present study, biomimetic magnetic nanoparticles (BMNPs) were synthesized with the mediation of MamC, a magnetosome protein from *Magnetococcus marinus* MC-1, and used to concentrate and detect bacteria. As a novelty compared to the existing biosensors based on MNPs, the surface characteristics of BMNPs allow a direct and efficient electrostatic interaction between microorganisms and nanoparticles without the need of post-production coating of BMNPs. Our results show that BMNPs, without any post-production functionalization, are very efficient binding both Gram positive and Gram negative bacteria and concentrating these microorganisms following upon the application of an external magnetic field. Once concentrated, the target microorganisms (*Staphylococcus aureus* used here as a model bacterium) can be specifically detected up to bacterial loads as low as 10 CFU/mL by using qPCR. Although the binding is unspecific, the specificity for detection is given by qPCR testing of the attached microorganisms. The system described here, without the need of functionalization, maintains (or improves) the detection limit for *S. aureus* compared to that obtained by using the Protocol ISO 6888–1:2022 and to that obtained by using antibody-functionalized MNPs, thus becoming a suitable, cost- and time-effective alternative for bacteria detection in fluid samples.

1. Introduction

The early detection of pathogenic microorganisms in food and/or water is of extreme importance, not only to avoid potential health risks, but to ensure safe food processing protocols in the relevant industries (Li et al., 2019). Therefore, the development of simple, cost-effective, accurate and sensitive procedures for the detection of pathogens is critical to accelerate treatments and to improve food security (Augustine et al., 2016; Houhoula et al., 2017). Many of the culture-dependent techniques traditionally used are time consuming, as the time for results depends on the growth of the relevant microorganism, usually being this resolution time above 24 h. When the contaminant microbial counts are very low, these techniques are also usually prone to false negative results, so pre-enrichment steps are usually required, increasing the resolution time even further. Therefore, there is room for developing novel, faster and more accurate protocols for the early detection of microbial contaminants in food and/or waters.

In this context, nanoparticles have become attractive components of biosensors compared to other conventional materials. They display a large surface to volume ratio that increase sensitivity, especially when decorated (functionalized) with molecules that can target specific microorganisms (Wang et al., 2011). Gold, silver and magnetic

* Corresponding author.
** Corresponding author.
*** Corresponding author.
E-mail addresses: mmartine@ugr.es (M. Martinez-Bueno), fvivas@ugr.es (A. Fernandez-Vivas), cjl@ugr.es (C. Jimenez-Lopez).

https://doi.org/10.1016/j.foodcont.2023.109623
Received 11 October 2022; Received in revised form 31 December 2022; Accepted 10 January 2023
Available online 13 January 2023
0956-7135/

nanoparticles (MNPs) are the ones most frequently used (Li et al., 2019), and, among them, MNPs are of special interest since, on top of the advantages above, they can be easily recovered by the application of an external magnetic field. By magnetically concentrating the MNPs, the attached microbial contaminant can also be concentrated, increasing the sensitivity of the biosensor. In this context, several authors have developed biosensors based on MNPs functionalized with antibodies with detection limits of ~10^2 CFU/mL (Table 1), although there are cases (Day & Basavanna, 2015) in which this detection limit reaches 10 CFU/mL. However, the lack of stability of the antibodies and their fairly high costs constitute drawbacks to these biosensors.

Therefore, the goal of the present study is to develop a biosensor that: (1) improves the performance and resolution time of the culture-dependent protocols defined in the Protocol ISO 6888–1:2022; (2) can be magnetically concentrated; and (3) avoids the use of antibodies, while maintaining the sensitivity already reached by the existing antibodies bearing-MNP biosensors.

With this goal in mind, a biosensor consisting of novel biomimetic magnetic nanoparticles of magnetite (BMNPs) is going to be designed. The novelty of BMNPs compared to traditional MNPs lies on changes on the size, magnetic properties, and composition of the former. These new characteristics of BMNPs are induced by the control over magnetite precipitation exerted by the protein MamC, a magnetosome-associated protein of *Magnetococcus marinus* MC-1, which is introduced in the reaction mixture. MamC controls BMNPs nucleation and growth acting as template for magnetite growth (Ubago-Rodríguez et al., 2019), which, in turn, results in superparamagnetic nanoparticles, larger (~35–40 nm) than those chemically produced (<20 nm). The size increase is important, not only in the context of surface area, but also to increase the magnetic moment per particle (Prozorov et al., 2013), which is important for an efficient response to the external magnetic field applied for concentration. Even with this size increase, BMNPs maintain their superparamagnetism, meaning that they behave as non-magnetic in the absence of an external magnetic field (preventing aggregation), but respond with a maximized magnetic susceptibility once an external magnetic field is applied (García Rubia et al., 2018).

Surface properties are also crucial to allow the interaction between nanoparticles and bacteria. Chemically produced MNPs usually present an isoelectric point (iep) of ~7 (García Rubia et al., 2018), and thus, any bonding based on electrostatic interactions, in particular, to the negatively charged microbial cell wall, is prevented at neutral pH values. Therefore, to allow interaction to the relevant microorganism, biosensors based on MNPs need to be functionalized with targeting molecules, such as antibodies (Table 1). Although this strategy may increase the sensitivity, it adds important disadvantages, mainly related to the cost and difficulty of handling antibodies, and the potential shield produced by the non-magnetic coating of the already non-optimal magnetic moment of the core, compromising an efficient magnetic concentration by an external magnetic field. However, BMNPs present an isoelectric point ~4.7 (García Rubia et al., 2018) due to the presence of MamC attached to the magnetic core, which provides functional groups that may allow an electrostatic interaction with the cell wall.

Based on BMNPs' properties, the hypothesis of the present study is that they can electrostatically bind microorganisms without the need of any functionalization, and concentrate them upon the application of an external magnetic field. As such, they could be potential candidates to produce easy handling, cost effective biosensors, provided that, although the binding is unspecific, the specificity for detection is given by qPCR testing of the attached microorganisms. Therefore, the present study aims, firstly, to analyze the potential of BMNPs to electrostatically bind Gram-positive bacteria (*Staphylococcus aureus* and *Enterococcus faecalis*, chosen as models) and Gram-negative bacteria (*Escherichia coli* and *Salmonella enteritidis*, chosen as models) without the need of functionalization with antibodies. Secondly, to test the potential of BMNPs to detect trace amounts of a specific bacterium (*S. aureus,* chosen as a model) in liquid media, by using qPCR for detection. Finally, as a third goal, the potential exits that residual traces of BMNPs remaining in the qPCR mixture could inhibit polymerase reaction and interfere with the protocol, so this issue is also analyzed and an optimized protocol for the qPCR analysis of this type of samples is here proposed.

Table 1
MNP-based biosensors.

Target	Limit of detection	Method	Reference
Staphylococcus aureus in PBS and milk	10^3 CFU/mL in PBS 10^5 CFU/mL in milk	Antibody nanocomposites synthesized by coating MNP (carboxylated MNPs, 100 nm) with bovine serum albumin, then adsorbing AuNPs and antibodies. Immunomagnetic separation (IMS) and colorimetric detection	Sung et al. (2013)
S. aureus in milk, blood and TSB *Salmonella enteritidis* in TSB and meat broth	1.5 × 10^2 CFU/mL (NP) 2 × 10° CFU/mL (MPIO)	MNP coated with polystyrene (MPIO, 1 μm) or dextran (NP, 60 nm) conjugated with antibodies PCR-based detection	Houhoula et al. (2017)
S. aureus in LB-Broth	2.3 × 10^2 CFU/mL	MNP-TiO2-AP-SMCC formed by: MNPs encapsulated by silica nanoparticles; TEOS (Tetraethoxysilane); APTES (3-aminopropyltriethoxysilane): SMCC (sulfosuccinimidyl 4-N-maleimidomethyl cyclohexane-1-carboxylate) The biosensor was added to a lysate of bacteria. Bacterial DNA was measured by using Nano-drop spectrophotometry.	Naderlou et al. (2020)
Escherichia coli O157 in food *Bacillus anthracis* in soil samples	*E. coli*: 10^2 CFU/mL ECL; 10^5 CFU/mL FCL *B. anthracis*: 10^3 CFU/mL ECL; 10^5 CFU/mL FCL	Antibody-coated MNPs. Immunodetection based on fluorogenic chemiluminescence, solid-phase chemiluminescence (FCL) and electrochemiluminescence (ECL)	Yu et al. (2000)
Listeria monocytogenes and *L. ivanovii* in infant formula and green leafy vegetables	*L. monocytogenes:* 10 CFU/mL (or g) *L. ivanovii*: 10 CFU/mL (infant formula); 10^2 CFU/g (leafy greens)	Antibody coated magnetic beads (Bio-Plex Pro Magnetic COOH beads). Bioluminiscence (Bio-Plex suspensión array system)	Day and Basavanna (2015)
Salmonella typhimurium and *S. aureus* in water	*S typhimurium:* 5 CFU/mL *S. aureus:* 8 CFU/mL	Aptamer-conjugated magnetic nanoparticles (amine-functionalized MNPs) plus aptamer-conjugated $NaYF_4$:Yb/Er, $NaYF_4$:Yb/Tm UCNPs. Bioluminiscence	Duan et al. (2012)
S. aureus, Micrococcus luteus, Bacillus cereus and *Streptococcus mutans* (viable cells)	33 CFU/mL	Vancomycin-coated carboxil-MNPs (2 μm) Bioluminescence (ATP determinations)	Su et al. (2017)
Salmonella spp. in milk	5 × 10^3 CFU/mL in LB; 7.5 × 10^3 CFU/mL in milk	Antibody-coated MNPs. Immunomagnetic separation and detection (IMS/m-GEC electrochemical immunosensing)	Liébana et al. (2013)
S. aureus in saline solution and milk	10^2 CFU/mL in saline solution; 10 CFU/mL in milk	Biomimetic magnetic nanoparticles. qPCR detection	This study

2. Materials and methods

2.1. Expression and purification of MamC. Synthesis and characterization of BMNPs

The expression and purification of MamC was carried out as described by Valverde-Tercedor et al. (2015). TOP10 strain of *E. coli* (Life Technologies: Invitrogen, Grand Island, NY, USA) was transformed with the 4.4 Kb pTrcHis-TOPO carrying *mamC* gene, allowing the expression of the MamC protein marked with a histidine tail at the N-terminal end. Once expressed, the protein was purified under Fast Protein Liquid Chromatography (FPLC) under denaturing conditions using an ÄKTA model FPLC system prime™ PLUS GoldSeal 2167311 (Ge Healthcare) and visualized by denaturing polyacrylamide gel electrophoresis (SDS-PAGE). Finally, the fractions containing MamC were allowed to refold at 4 °C by dialysis using 1 L of dialysis buffers A (Tris 50 mM, NaCl 150 mM, urea 6 M, pH 8.5) and B (Tris 50 mM, NaCl 150 mM, pH 8.5) as starting and end points, respectively.

The biomineralization experiments followed the procedure and guidelines described by Perez-Gonzalez et al. (2011) and Valverde-Tercedor et al. (2015). The nanoparticles were obtained by adding MamC (in a final concentration of 10 μg/mL) to a master solution composed of deoxygenated solutions of $NaHCO_3$, Na_2CO_3, $Fe(ClO_4)_2$ and $FeCl_3$ in a final concentration of 3.5 mM, 3.5 mM, 2.78 mM and 5.56 mM, respectively, added with NaOH to reach pH 9. The deoxygenated solutions were prepared with O_2-free MilliQ water, obtained by boiling MilliQ water for 1 h and cooling it in an ice bath while continuously sparging with ultrapure N_2. The master solution was incubated for 30 days at 25 °C and 1 atm of total pressure inside an anaerobic chamber (Coy Laboratory Products, Grass Lake, MI). The nanoparticles formed were washed with O_2-free MilliQ water three times by magnetically concentrating the solid, removing the clear supernatant and adding fresh water in each cycle. To measure the concentration of BMNPs, 1 mL of the batch was withdrawn and placed in 1.5 mL microfuge tube (Eppendorf) previously weighted in a precision balance (Analytical Balance 220 g × 0.1 mg Radwag AS 220/C/2). The nanoparticles were magnetically concentrated and the supernatant was removed. The tube containing BMNPs was placed in a dry bath (AccuBlock™ Digital Dry Bath, Labnet) at 95 °C for 30 min until the nanoparticles were completely dried. The tube was removed for the dry bath and cooled to room temperature. Then, it was weighted in the precision weight scale. The weight of the BMNPs in each specific tube was calculated as the weight difference between that of the tube containing the dry solid and that of the same empty tube. A minimum of five replicas were performed. Then, the supernatant of the batch was removed and the BMNPs were resuspended in deoxygenated water to reach a concentration of 15 mg/mL. Finally, the BMNPs were autoclaved (121 °C, 15 min) and stored at 4 °C.

Powder X-ray diffraction (XRD) analysis was carried out with an Xpert Pro X-ray diffractometer [PANalytical (CuKα-radiation, 20 to 60° in 2θ (0.01°/step; 3s per step)]. The size of BMNPs was determined from micrographs taken by transmission electron microscopy [TEM; LIBRA 120 PLUS (Carl Zeiss SMT), equipped with Electron Energy Loss Spectroscopy, EELS]. The nanoparticles were embedded in Embed 812 resin, and ultrafine sections (50–70 nm) were obtained with a Reichert Ultracut S microtome (Leica Microsystems GmbH, Wetzlar, Germany) and deposited in copper nets. The size of the crystals was manually measured using the ImageJ 1.47 program, and size distribution curves were determined from these measurements using Origin 8. Since the 2D-section of the crystals were rectangles or rhombs (showed in Results and Discussion section), the measurement of the larger edge was considered, and only crystals with well-defined edges were counted, to avoid size overestimation due to aggregation. To ensure reproducibility of results, particle sizes were measured on multiple micrographs with an accumulated amount of about 1000 nanoparticles measured for each experiment. The isoelectric point of BMNPs was determined from the calculation of ζ-potential based on electrophoretic mobility measurements (viscosity: 0.8872 cP, dielectric constant: 78.5, temperature: 25 °C), which were carried out in a Zetasizer Nano-ZS [Malvern Instruments, Malvern, UK] at 25 °C as detailed by García Rubia et al. (2018).

2.2. BMNPs as bacterial magnetic concentrating agents

The potential of BMNPs to bind bacteria was evaluated by mixing suspensions of BMNPs in oxygen free water, within a concentration range from 0 to 2.5 mg/mL (0, 0.1, 0.25, 0.5, 1 and 2.5 mg/mL), with cell cultures of the bacteria listed below (cell concentrations of 10^3, 10^2 and 10 CFU/mL for each cell type). The bacteria used for the test were both Gram-positive (*S. aureus* ECT240 and *E. faecalis* LMG0822) and Gram-negative (*S. enteritidis* LMG7233 and *E. coli* LMG8223). All trials were replicated three times.

All bacteria were first grown on Trypto-Casein Soy Agar plates (TSA, commercial preparation of Scharlau) and incubated at 37 °C for 24–48 h. Then, colonies were resuspended in sterile 0.9% NaCl solution until reaching a turbidity corresponding to the order of 10^8 CFU/mL according to the McFarland scale. From this suspension, serial decimal dilutions were made in sterile 0.9% NaCl to obtain suspensions containing 10^3, 10^2 and 10 CFU/mL. The concentration of each one of these dilutions was quantified by counting the colonies grown on TSA.

For each type of bacteria, electrophoretic mobility measurements were performed on a suspension containing 10^3 CFU/mL of the relevant bacteria in 0.9% NaCl, by using a Zetasizer Nano-ZS [Malvern Instruments, Malvern, UK] at 25 °C. ζ-potential was calculated from these measurements (viscosity: 1.01 cP, dielectric constant: 78, temperature: 25 °C).

Different volumes of the BMNPs stock were withdrawn to prepare a series of tubes in which the final concentration of BMNPs ranged from 0 to 2.5 mg/mL. In each tube, BMNPs were magnetically concentrated and the supernatant was discarded. For each bacterial type, six sets of samples were prepared (9 microfuge tubes each, which included three experiments in triplicate), each containing the following mg of BMNPs: (1) 0 mg (control), (2) 0.1 mg, (3) 0.25 mg, (4) 0.5 mg, (5) 1 mg, and (6) 2.5 mg. All tubes were filled with 1 mL of the relevant bacterial suspension (x3): (A) 10^3 CFU/mL, (B) 10^2 CFU/mL, (C) 10 CFU/mL. The pH value of all these mixtures was 6.2. Adsorption experiments cannot be done at acidic pH values because of the potential BMNPs dissolution.

All the mixtures were placed for 30 min in a Mini LabRoller™ Rotator (Labnet) and then, the samples were placed on a 16-Tube SureBeads™ Magnetic Rack (Bio-Rad) for 30 min to ensure total magnetic concentration of the solid. Then, while the solid was kept magnetically concentrated, the supernatant was removed. The solid pellets were analyzed by TEM and EELS.

The supernatant was diluted in 20 mL of sterile distilled water, and filtered (0.45 μm; EZ-Pak™ Membrane Filters, Millipore). All the filter membranes were immediately deposited on TSA plates and incubated at 37 °C for 24 h. After this time, a count was made of the colonies grown on each filter (X_n). The count obtained in the experiment set #1 (BMNP-free) at each bacterial concentration (X_0) was used as a reference to determine the percentage of bacteria retained by the BMNPs, using equation (1).

$$\textit{Retention percentage}\ (\%) = \frac{X_0 - X_n}{X_0} \times 100 \tag{1}$$

2.3. Detection of the magnetically concentrated bacteria by qPCR

S. aureus ECT240 was used as a model bacterium to determine, by qPCR, the detection limit of the sensor after the electrostatic binding of this bacterium to BMNPs and following magnetic concentration. qPCR was used for the selective detection. Firstly, a calibration curve was performed, and then, the potential of inactivation of the polymerase due to the presence of BMNPs was investigated, these protocols detailed below. Finally, a protocol was developed to optimize the bacterial detection.

Serial dilutions from a culture of *S. aureus* ECT240 (10^8 CFU/mL) from 10^6 to 10 CFU/mL were prepared in 0.9% NaCl to obtain a qPCR calibration curve. DNA extraction was performed following the rapid lysis method of Boom et al. (2000). qPCR was done using a CFX Connect Real-Time PCR Detection System (BIORAD) for the quantification of the bacterium. The amplicon was purified following the indications of the GenElute™ PCR Clean-Up Kit. Amplifications were performed at a final volume of 20 μL containing 2 μL of DNA template, 0.3 μM final concentration of each primer [Sa442-1 (AATCTTTGTCGGTACACGA-TATTCTTCAC) and Sa442-2 (CGTAATGAGATTTCAGTTAGATAA TACAAC)] (Martineau et al., 1998), 10 μL of Master Mix [TB Green Premix Ex *Taq*II (Tli RNase H Plus)-TAKARA] and Milli-Q water up to 20 μL. The amplification was run in 40 cycles, starting with an initial denaturation at 95 °C for 30 s followed by 40 cycles at 95 °C for 5 s and 63 °C for 30 s. The efficiency of the reaction was calculated from the slope of the standard curve ($R^2 > 0.98$) using equation (2). To evaluate the intra- and interassay reproducibility, the coefficient of variation (CV) was also calculated.

$$Efficiency = 10^{\frac{-1}{slope}} - 1 \tag{2}$$

The data were statistically analyzed with R Studio Statistics. Comparisons were carried out with a one-way analysis of variance and post hoc Tukey's honestly significant difference. Differences with P values lower than 0.05 were considered statistically significant. The reproducibility, amplification efficiency and coefficient of linearity of the standard curves in qPCR were found to be consistent. The qPCR validation was done by visualizing the dissociation temperature profiles, which confirmed specific amplification.

2.3.1. Optimization of DNA extraction protocol for BMNP-bearing samples. Analysis of the potential interference of BMNPs with qPCR

An adsorption experiment was done using *S. aureus* ECT240 as a model strain, in the presence of 0.5 mg/mL of BMNPs. Briefly, serial dilutions of *S. aureus* from 10^6 to 10 CFU/mL were prepared in 0.9% NaCl and added with 0.5 mg/mL of BMNPs in a total volume of 1 mL. Adsorption experiments were performed as indicated in subsection 2.4 and the pellet was magnetically collected (these samples are here referred as BMNP-bearing samples). As a control experiment (BMNP-free), a set of dilutions of *S. aureus* were prepared from 10^8 to 10^2 CFU/mL from which 10 μL each were withdrawn (thus containing from 10^6 to 10 CFU). The experiment was replicated three times.

DNA extraction was performed following the protocol in Boom et al. (2000) to which some modifications were included to optimize the lysis and DNA extraction in BMNP-bearing samples. 50 μL of lysis solution were added to the samples. At this point, replica were done to test the effect of sonicating these samples on DNA extraction efficiency. The rationale behind was that following upon bacterial lysis, DNA could electrostatically bind to BMNPs, compromising the efficiency of the extraction protocol. No sonication (0 min), 1, 3 and 5 min sonication were tested on samples after adding the lysis solution, using an EMMI®-30HC Ultrasonic cleaner (180 W, 220–240 V, 50–60 Hz, EMAG Germany). All samples were incubated for 10 min at 90 °C and cooled to room temperature. Afterwards, a volume of 50 μL of neutralization solution was added. Then, in case of the BMNP-bearing samples, BMNPs were magnetically separated from the supernatant, which was collected and stored at 4 °C for qPCR analysis. qPCR was performed as detailed in subsection 2.5.1.

2.4. Detection limit of magnetically concentrated S. aureus by qPCR

Two types of experiments were done in two different matrixes (saline solution and milk) to determine the detection potential of BMNPs using *S. aureus* ECT240 as a model strain. The first set is here referred as BMNP-bearing and the second one as ISO experiment. For both types of experiments, suspensions of *S. aureus* from 10^3 CFU/mL to 1 CFU/mL were prepared in saline solution (0.9% NaCl) or in milk matrix.

Type 1: BMNP-bearing experiment. Aliquots of 1 mL of the suspensions of *S. aureus* (10^3 CFU/mL, 10^2 CFU/mL, 10 CFU/mL and 1 CFU/mL) were added (x3) to tubes containing 1 mg BMNPs prepared following the protocol detailed in subsection 2.4. All the samples were placed in the Mini LabRoller™ Rotator (Labnet) for 30 min and then, placed in the magnetic rack for 30 min for BMNPs concentration. The BMNPs from each tube were collected for DNA extraction and qPCR analyses. Identical experiments were performed for each matrix (saline solution or milk).

Type 2: ISO experiment. Aliquots of 100 μL from each suspension of *S. aureus* with concentrations of 10^3 CFU/mL, 10^2 CFU/mL, 10 CFU/mL and 1 CFU/mL (both in saline solution and milk) were spread on plates of Baird Parker medium (Scharlau) with potassium tellurite (Scharlau), incubated at 37 °C for 24–48 h.

Additional experiments were performed by centrifuging 1 mL of the sample for 10 min at 6000×*g* and 4 °C. This protocol became unbearable when the matrix was milk. In this case, a solid butter was obtained that prevented further sampling for PCR analyses. Therefore, this procedure was not used in the present manuscript.

3. Results and discussion

3.1. BMNP as bacterial magnetic concentrating agents

BMNPs were composed of magnetite (>95%) according to XRD analyses. TEM microphotographs show well-defined crystal faces and a 2D rectangular and rhomboidal shape (Fig. 1A). Their size ranges between 10 and 60 nm, although ~60% of BMNPs show a size of 25–35 nm (Fig. 1B). The average size is 34 ± 6 nm. BMNPs have an isoelectric point of 4.4, being positively charged at lower pH values and negatively charged at higher pH values (Fig. 1C).

Given the comparative size of BMNPs (in the nano range, Fig. 1) and bacteria (in the micro range), BMNPs, individually and/or aggregated, bind to the cell wall or the extrapolymeric substances (EPS) (Fig. 2). Once attached, the assembly becomes magnetic and can be concentrated following upon the application of an external magnetic field (Fig. 4).

BMNPs are, in fact, nanocomposites containing a magnetite core and MamC attached to (or even incorporated into) the outer layers of this magnetic core, conferring new surface functional groups. These functional groups are responsible for the surface charge of BMNPs, as the measured iep (4.4, Fig. 1C) is that of the MamC protein (García Rubia et al., 2018). BMNPs present carboxylic, hydroxyl and amine groups (García Rubia et al., 2018), while bacteria have a negatively charged cell wall conferred by lipoteichoic acids and teichoic acids in Gram-positive bacteria (such as *S. aureus* and *E. faecalis*) and lipoproteins, membrane proteins and lipopolysaccharides (LPS) in Gram-negative bacteria (such as *E. coli* and *S. enterica*). In fact, ζ-potential of the bacterial culture determined at pH 6.2 shows that all exhibit negative surface charge (Fig. 3), with no significant differences between them (ANOVA test p-value >0.05). Other external bacterial structures, as EPS secreted by *S. aureus,* also provide functional groups able to electrostatically interact with BMNPs (Dragoš & Kovács, 2017; Hou et al., 2017).

Taking into account the relative size difference (micro versus nano) between bacteria and BMNPs, surface charge of either of them cannot be considered as a bulk, as determined from electrophoretic measurements, but the interaction between the bacteria and BMNPs have to be narrowed to a much smaller scale. On one hand, electrostatic interaction between bacteria and BMNPs may occur either between the amine groups present in MamC at BMNPs surface and the negatively charged groups at the bacteria cell wall and/or between the carboxylic/hydroxyl groups of MamC at BMNPs surface and amine groups present in EPS. It has to be also considered that the presence of cations (such as Na^+ in

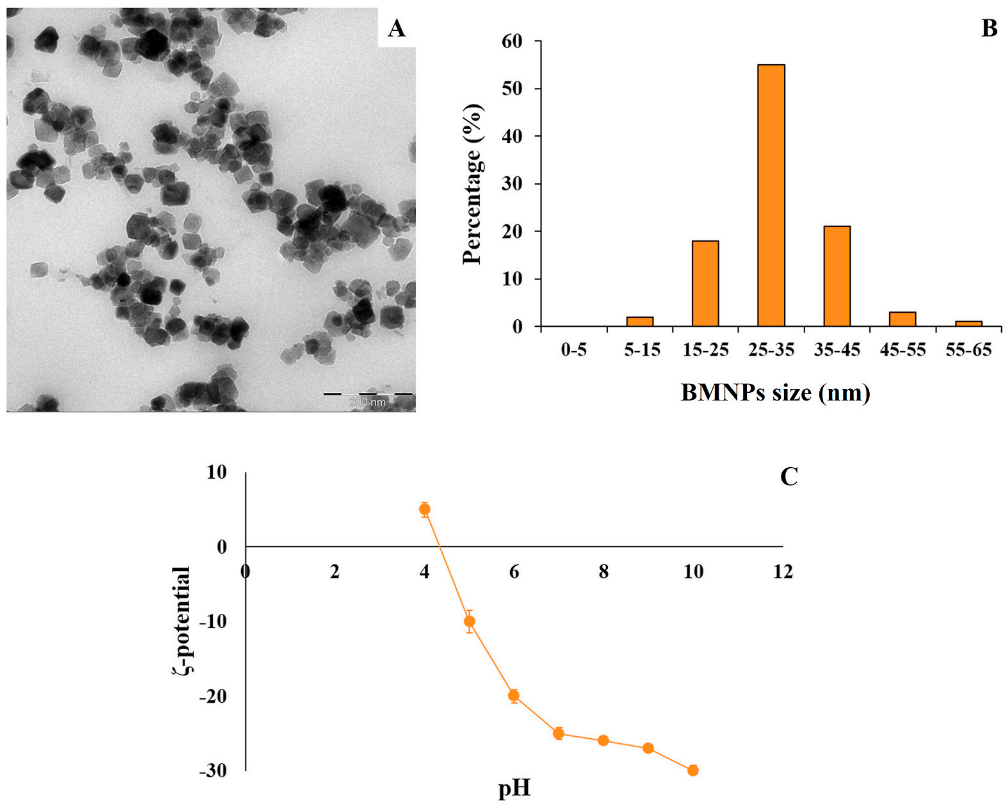

Fig. 1. Characterization of BMNPs. (A) TEM micrograph (scale bar: 200 nm). (B) Size distribution. (C) ζ-potential.

saline solution and Ca^{2+} in milk) may act as "bridges" between negatively charged residues in both bacteria and BMNPs. Moreover, hydrophobic interactions cannot be ruled out between the phospholipids bilayer, forming the outer cell membrane in Gram-negative bacteria, and the MamC transmembrane domains (hydrophobic). Therefore, the type of interaction (whether it is hydrophobic or electrostatic), and the number and availability of the exposed functional groups both in BMNPs and in the bacterial outer structures, anticipate differences in their binding to BMNPs and, as a result, in the efficiency of the magnetic concentration. In any case, these interactions confer "magnetic properties" to the bacteria that allow their magnetic recovery, as shown in Fig. 4.

According to the results in Fig. 4, the magnetic concentration of BMNPs allows the recovery of the bacterial cells from the mixture, in a percentage that varies with the ratio [BMNPs]/bacterial load. For a given inoculum concentration, the higher the concentration of BMNPs, the higher the retention percentages (Fig. 4). To achieve a retention percentage of 100% of *S. aureus* (inoculum concentration from 10 to 10^3 CFU/mL), 0.25 mg/mL of BMNPs were enough, while lower BMNP concentrations failed. This amount (0.25 mg/mL of BMNPs) was enough to retain up to 10^2 CFU/mL of *E. faecalis*, but when the inoculum concentration was 10^3 CFU/mL, the concentration of BMNPs had to increase to 0.5 mg/mL to retain 100% of the inoculum. For Gram negative bacteria, higher concentrations of BMNPs were needed to retain 100% of the inocula. In fact, 1 mg/mL of BMNPs was needed to retain 100% of *E. coli* (inoculum concentration from 10 to 10^3 CFU/mL), while even 2.5 mg/mL of BMNPs were not enough to retain 100% of *S. enteritidis* inoculum (10–10^3 CFU/mL).

While, except in the case of *S. enteritidis*, no significant differences in bacterial retention percentages are observed at high concentrations of BMNPs irrespectively of the bacterial load, large variations in these retention percentages were observed at low concentrations of BMNPs, specially for the more diluted bacterial loads (10 CFU/mL), which is especially evident for Gram-negative bacteria (Fig. 4C and D). These large variations may be related to the difficulty of BMNPs and bacteria to meet and then interact in such a diluted system and/or to the fact that the amount of BMNPs is not enough to mediate an efficient magnetic concentration of the cells. This problem is solved when the concentration of BMNPs is increased.

It is also observed that lower concentrations of BMNPs are needed to recover ~100% of the Gram-positive bacteria to that needed to recover this percentage of Gram-negative bacteria. Other than differences in binding due to the different composition in the outer structures between Gram-positive and Gram-negative bacteria, these variations in the retention percentages might also be related to the ability of the former to form bacteria clusters. Our hypothesis is that the formation of bacterial clusters (especially evident in *S. aureus* and in *E. faecalis*) increases the efficiency of the magnetic recovery, going from cluster magnetic concentration to individual magnetic concentration if cells do not form clusters (as it is the case of the Gram-negative bacteria tested).

Other factors are also important in the context of the magnetic concentration of cells mediated by BMNPs, as differences in bacteria surface charge and/or the type, distribution and orientation of the surface functional groups. In fact, the retention percentage observed for *E. coli* and *S. enteriditis* are different, that may be related to differences in the LPS (number and composition of functional groups) found between these two bacterial species (Bhunia, 2018a, 2018b; Meysman et al., 2013; Samuel & Reeves, 2003; Stenutz et al., 2006). This hypothesis agrees with the findings of some authors (Jacobson et al., 2015), which related the successful electrostatic interaction of gold nanoparticles (AuNPs) with *Shewanella oneidensis* depending on LPS content. They observed that electrostatic interactions between cationic AuNPs and the outer membranes were favored the higher was the LPS content in the outer membrane. In addition, they suggested that O antigen played a role in this interaction. Actually, this O antigen is one of the cell structures in which differences have been also found between *E. coli* and *S. enterica* (Meysman et al., 2013), which further supports our hypothesis that composition and distribution of functional groups in outer cell

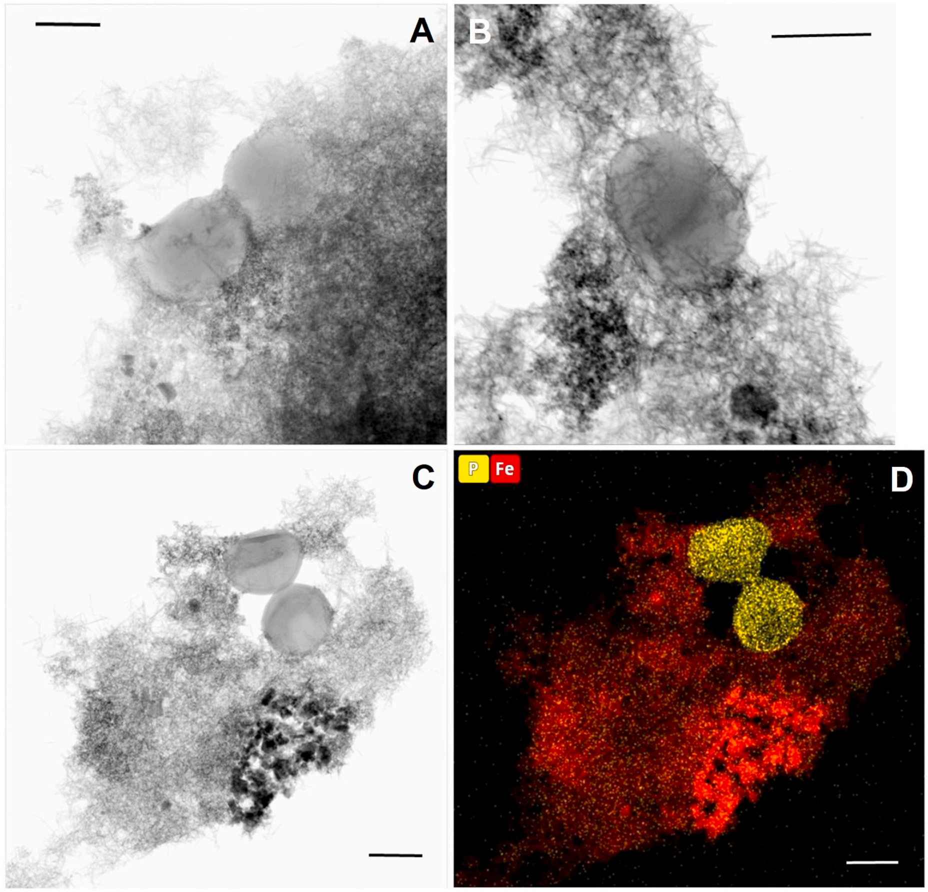

Fig. 2. BMNPs attached to *S. aureus* cells. (A, B, C) TEM images. (D) Compositional EELS map of Fig. 2C; Fe (red) from BMNPs and P (yellow) from cells are shown. Scale bars: 500 nm.

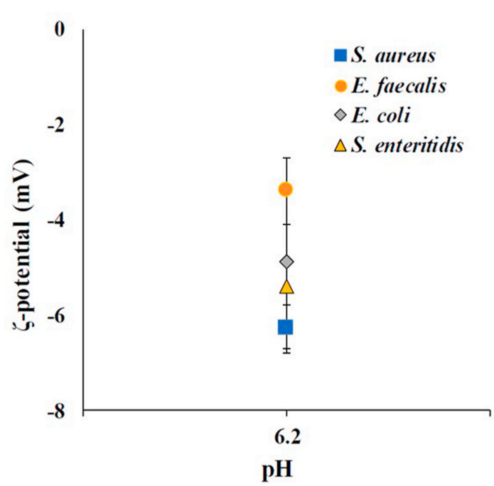

Fig. 3. ζ-potential of bacteria at pH **6.2.**

structures may determine the ability to be magnetically concentrated by BMNPs.

In any case, it is important to point that our results show that BMNPs are able to mediate the effective magnetic recovery of both Gram-positive and Gram-negative bacteria, even at the lower bacterial loads tested (10 CFU/mL) and, even more, without the need to be functionalized with an antibody or any other targeting molecule. This represents a relevant step forward compared to existing biosensors based on magnetic nanoparticles (Tables 1 and i.e., Bülbül et al., 2015; Houhoula et al., 2017; Li et al., 2019; Yuan et al., 2014).

3.2. Detection of the magnetically concentrated bacteria by qPCR

3.2.1. Optimization of DNA extraction protocol for BMNP-bearing samples. Analysis of the potential interference of BMNPs with qPCR

Once the BMNP pellet was recovered from the bacterial cultures and DNA extraction was attempted, following upon bacterial lysis, an electrostatic interaction may occur between DNA and BMNPs, that reduces the amount of DNA copies left in the supernatant after magnetic separation of the BMNPs. Therefore, after the lysis procedure, the mixture was sonicated for different time intervals to disrupt this potential electrostatic interaction between DNA and BMNPs. In fact, Fig. 5 proves our hypothesis and shows that the amount of DNA in the supernatant (once BMNPs are removed), following upon cell lysis increases with sonication time. These data demonstrate that the DNA was, in fact, interacting with BMNPs. The interaction between DNA and BMNPs is electrostatic. When the sample is sonicated, BMNPs are shaken and the solution slightly heats up. It has been previously shown that BMNP movement and the associated increase in thermal energy triggers a fast release of molecules previously electrostatically bound to BMNPs. Thermal energy disrupts the electrostatic binding and the molecule previously bound is released. This conclusion has been tested in numerous occasions by using BMNPs as a substrate and the following molecules electrostatically bound to them: DOXO (Jabalera et al., 2020; Peigneux et al., 2019) and choline kinase alpha inhibitors (Jabalera et al., 2019). In these cases, BMNPs movement and thermal energy increased was attained by magnetic hyperthermia. The higher the thermal energy (that occurring at the highest sonication times), the more successful is the weakening of the electrostatic bond DNA-BMNPs and higher amount of DNA is released.

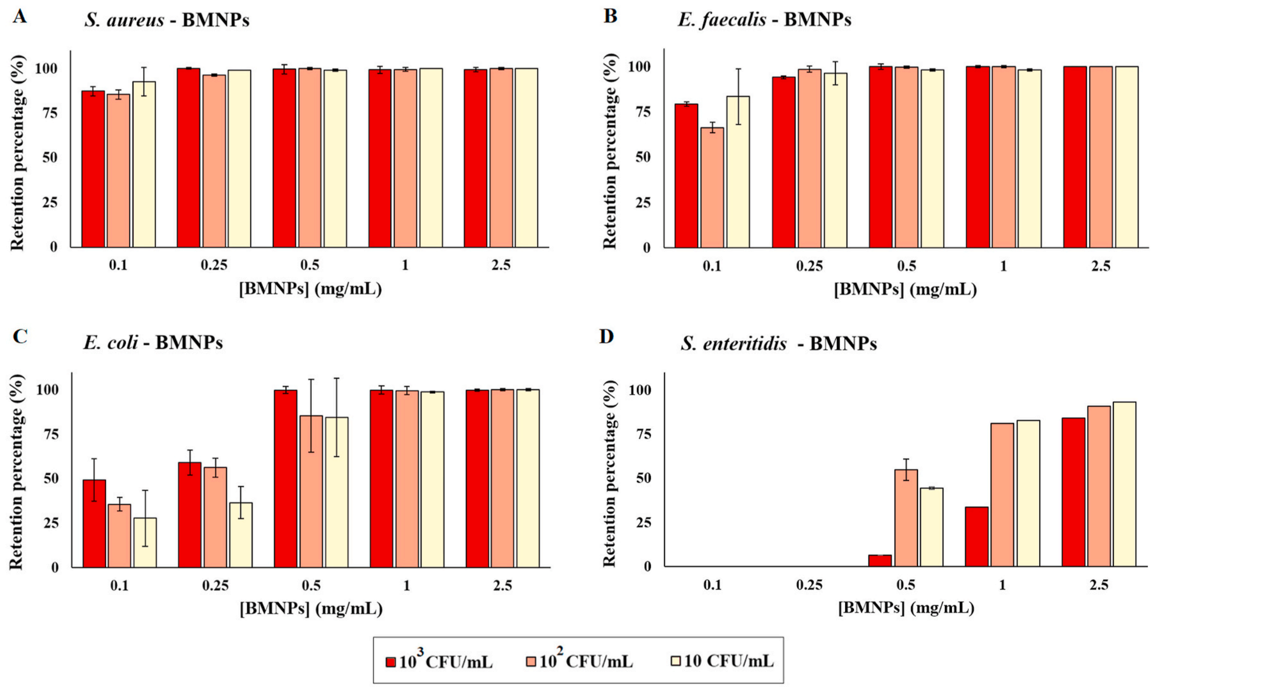

Fig. 4. Magnetic recovery of bacteria. Retention percentage (%) of (A) *S. aureus*, (B) *E. faecalis*, (C) *E. coli* and (D) *S. enteritidis* after magnetic concentration, following mixing with BMNPs concentration ranging between 0.1 and 2.5 mg/mL. The bacterial load in the mixture was 10^3, 10^2 and 10 CFU/mL (bright red, soft red and yellow, respectively).

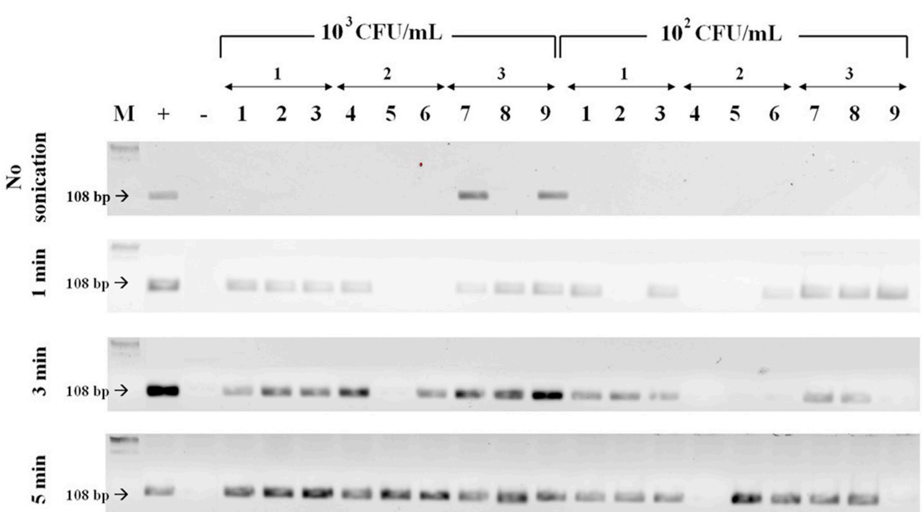

Fig. 5. Optimization of DNA extraction protocol. *S. aureus* DNA fragment amplification at different sonication times, following upon cell lysis, from the supernatant once BMNPs (0.5 mg/mL) were magnetically concentrated and removed. M: Lambda DNA/*Hind*III marker; +: positive control; -: negative control; 1–9: experiments containing 10^3 CFU/mL [1–3: replica #1 (x3); 4–6: replica #2 (x3); 7–9: replica #3 (x3)]; 10–18: experiments containing 10^2 CFU/mL [10–12: replica #1 (x3); 13–15: replica #2 (x3); 16–18: replica #3 (x3)].

Based on the results, the qPCR reaction protocol was modified to account for this artifact, as to include 5 min of sonication after the lysis protocol as a compromise to reach maximum desorption while avoiding potential DNA degradation. To avoid DNA readsorption into BMNPs, aliquots to continue qPCR reaction were taken immediate after sonication.

The potential interference of BMNPs with qPCR reaction was studied by comparing the qPCR results of two types of lysates with identical bacterial load: one of them withdrawn from a culture of *S. aureus* (control), and the other from the BMNPs pellets magnetically concentrated from a mixture with *S. aureus* (BMNP-bearing). As shown in Fig. 6, there are no significant differences in the C_q value between the control and BMNP-bearing experiments for any bacterial load, showing that BMNPs do not interfere with qPCR reaction.

3.2.2. Evaluation of BMNPs as a bacterial sensor: detection limit by qPCR

Dilute suspensions of *S. aureus* (10^3, 10^2, 10 and 1 CFU/mL), used as model microorganism (both in saline solution and milk), were mixed with 1 mg/mL of BMNPs, according to the procedure described in subsection 2.6. After magnetic concentration of the pellet, the supernatant was plated to determine the retention percentage, which was ~100% when the matrix was saline solution, and lower (~90%) when the matrix was milk. This is expected as any charged molecule in the milk interferes with the charged functional groups present both at the cell outer structures and in BMNPs, lowering the efficiency of the cell-BMNP interaction. DNA extraction and qPCR detection were performed on the pellets of all these experiments and the results are shown in Fig. 7 for saline solution as matrix, and in Fig. 8 for milk as matrix.

Although agarose gels were enough to account for the detection of the relevant bacteria, the potential exist that artifacts could provide false

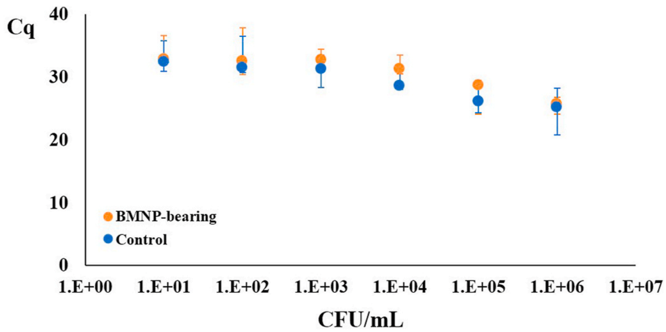

Fig. 6. Analysis of potential interference of BMNPs with qPCR. Cq values for different bacterial loads of *S. aureus* in BMNP-bearing and control experiments.

positive results. In fact, the PCR product is small (108 bp) and long amplification cycles were used. Therefore, qPCR was preferred to ensure that the amplified product was correct and not the result of non-specific amplifications or artifacts resulting from the dimers-primer that could be generated in long amplification cycles. The qPCR technique makes it possible to generate an amplicon that can be visualized in gels, but also to determine that it is specific on basis of melting temperature (76 °C). This test is especially important when the concentrations of cells to be detected are very low, as those used in the present experiments $< 10^3$ CFU/mL.

In BMNP-bearing experiments, 100% success in *S. aureus* detection in saline solution was obtained at bacterial loads of 10^2 CFU/mL and consistently decreased (64% success and 34% success) at lower bacterial loads (10 and 1 CFU/mL, respectively). Therefore, even 1 CFU/mL could be detected, but this detection occurred in only one of the three replica. Thus, the limit of detection was set at 10^2 CFU/mL, as positive results were obtained for all the replica at this concentration. When milk was the matrix in which *S. aureus* was suspended, a 100% success in the detection of this bacteria was achieved at bacterial loads of 10 CFU/mL, and a 64% success was achieved at bacterial loads of 1 CFU/mL. Identically as earlier, we set the limit of detection at 10 CFU/mL because positive results were obtained in all the replica. Regarding the experiment performed following the Protocol ISO 6888–1:2022, other than the disadvantage of the resolution time (24–48 h), growth was only detected when the bacterial load was $\geq 10^2$ CFU/mL. No growth was detected in plates at lower bacterial loads in any of the replica performed.

These results show that unequivocal *S. aureus* detection is improved, in both resolution time and detection limit, following magnetic concentration by BMNPs compared to that achieved by following the protocol described in Protocol ISO 6888–1:2022.

Several sensors based on nanoparticles have already been proposed for the detection of bacteria in different matrixes, related to environmental, food, clinical and pharmacological samples. Table 1 shows some of these sensors based on Fe-rich magnetic nanoparticles. In all cases, the nanoparticle is covered with an antibody (or other molecules) that provides functional groups for the interaction of the nanoparticles with the target. This is one of the most striking differences with the sensor proposed in the present study, as no further coating of BMNPs are needed. The advantage of the covering for the previous sensors is the specificity that the antibody brings to the detection, which allows the use of a variety of techniques for revealing this interaction sensor-microorganism, such as colorimetry (Sung et al., 2013), immunodetection (Sung et al., 2013; Yu et al., 2000; Liébana et al., 2009), bioluminescence (Day & Basavanna, 2015; Duan et al., 2012; Su et al., 2017), chemiluminescence (Yu et al., 2000) and/or electrochemiluminescence (Yu et al., 2000). The main disadvantages are, on one hand, the stability of the nanocomposite and, on the other, the need of a post-production coating, which obviously increases time and cost for the production of the sensor and may shield the magnetic core, somehow compromising the efficiency of the magnetic recovery.

Regarding limits of detection for *S. aureus*, the detection limit for *S. aureus* obtained by using BMNPs (~10 CFU/mL) compares very well and even improves those reported for antibody-functionalized MNPs biosensors (Table 1). The use of the antibody-functionalized gold coated magnetic nanoparticles produced by Sung et al. (2013) allows the detection of 10^5 CFU/mL in milk samples and 10^3 CFU/mL in PBS. This detection limit improves to 10^2 CFU/mL by using the

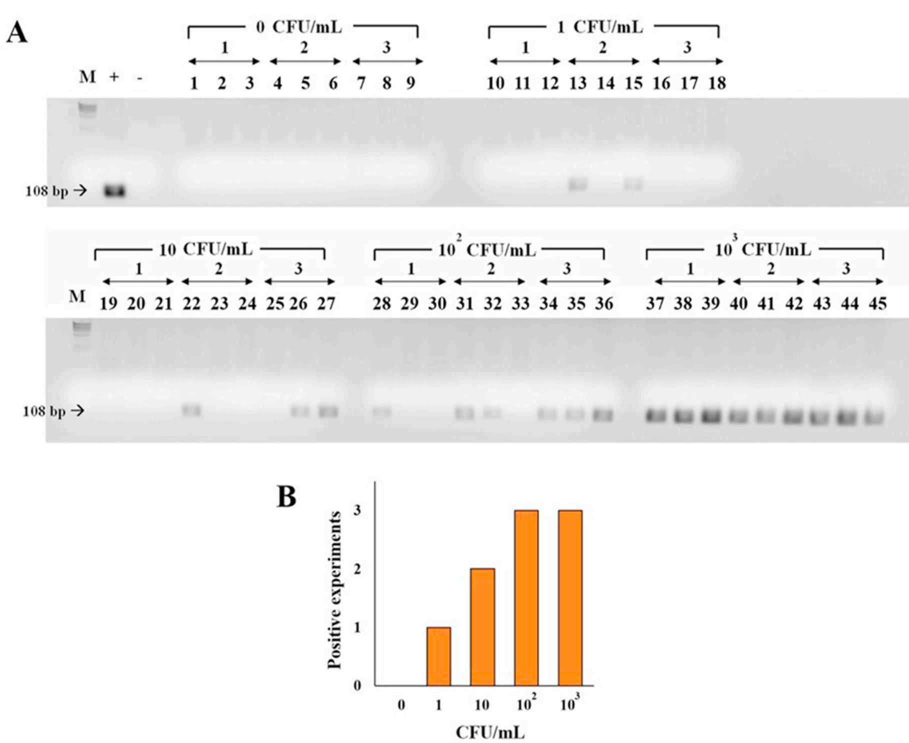

Fig. 7. qPCR of the samples collected from magnetically concentrated pellets of BMNPs from a suspension of *S. aureus* in saline solution 0.9% (BMNP-bearing). (A) Agarose gel electrophoresis. M: Lambda DNA/*Hind*III marker; +: positive control; -: negative control; 1–9: experiments containing 0 CFU/mL [1–3: replica #1 (x3); 4–6: replica #2 (x3); 7–9: replica #3 (x3)]; 10–18: experiments containing 1 CFU/mL [10–12: replica #1 (x3); 13–15: replica #2 (x3); 16–18: replica #3 (x3)]; 19–27: experiments containing 10 CFU/mL [19–21: replica #1 (x3); 22–24: replica #2 (x3); 25–27: replica #3 (x3)]; 28–36, experiments containing 10^2 CFU/mL [28–30: replica #1 (x3); 31–33: replica #2 (x3); 34–36: replica #3 (x3)]; 37–45, experiments containing 10^3 CFU/mL [37–39: replica #1 (x3); 40–42: replica #2 (x3); 43–45: replica #3 (x3)]. (B) Number of positive experiments out of the three performed replica (3 positives = 100% success, 2 positives = ~67% success, 1 positive = ~34% success).

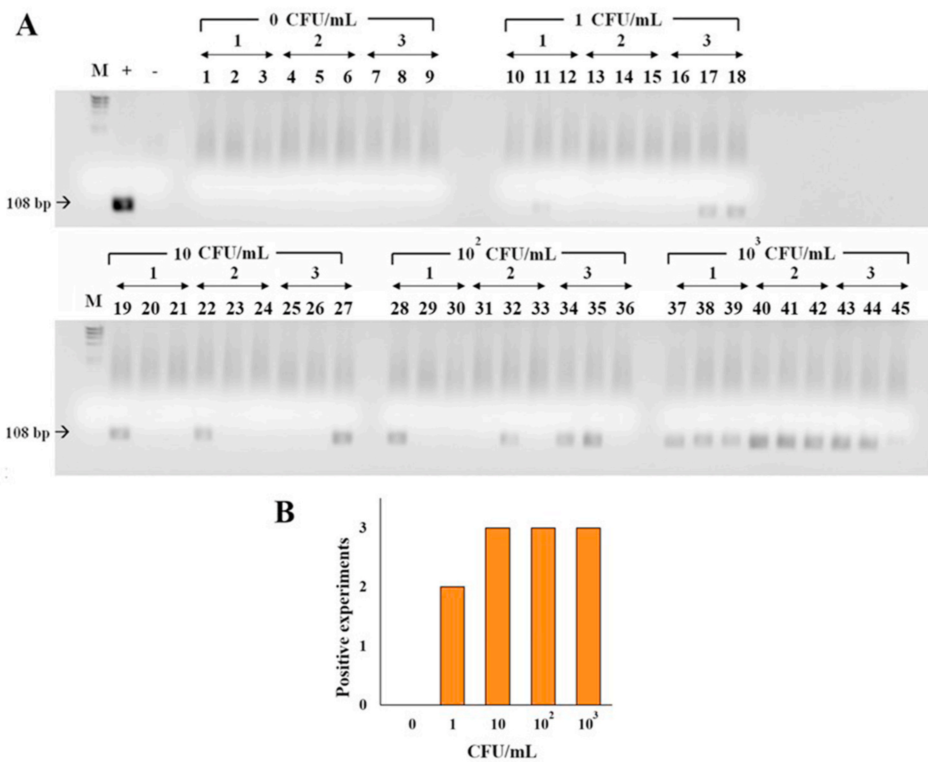

Fig. 8. qPCR of the samples collected from magnetically concentrated pellets of BMNPs from a suspension of *S. aureus* in milk (BMNP-bearing). (A) Agarose gel electrophoresis. M: Lambda DNA/*Hind*III marker; +: positive control; -: negative control; 1–9: experiments containing 0 CFU/mL [1–3: replica #1 (x3); 4–6: replica #2 (x3); 7–9: replica #3 (x3)]; 10–18: experiments containing 1 CFU/mL [10–12: replica #1 (x3); 13–15: replica #2 (x3); 16–18: replica #3 (x3)]; 19–27: experiments containing 10 CFU/mL [19–21: replica #1 (x3); 22–24: replica #2 (x3); 25–27: replica #3 (x3)]; 28–36, experiments containing 10^2 CFU/mL [28–30: replica #1 (x3); 31–33: replica #2 (x3); 34–36: replica #3 (x3)]; 37–45, experiments containing 10^3 CFU/mL [37–39: replica #1 (x3); 40–42: replica #2 (x3); 43–45: replica #3 (x3)]. (B) Number of positive experiments out of the three performed replica (3 positives = 100% success, 2 positives = ~67% success, 1 positive = ~34% success).

antibody-conjugated magnetic nanoparticles covered with dextran proposed by Houhoula et al. (2017) or even to 2 CFU/mL if those MNPs were covered with polystyrene instead. The nanocomposite used by Naderlou et al. (2020) was able to detect ~10^2 CFU/mL, but the formulation of the sensor was very complicated (Table 1). Su et al. (2017) reached a limit of detection of 33 CFU/mL, but still, their nanosensor needed a double post-production coating of carboxyl first and then vancomycin. Other sensors have been proposed for the detection of other microorganisms (Table 1), and, while their limits of detection compare well with the sensor proposed here, their formulation is more complex and post-production coating is always required. The sensor proposed here has the advantage that BMNPs do not require any post-production coatings, which, on top of ease the production process, does not pose any potential shielding of the magnetic core, allowing a more efficient magnetic concentration. The specificity for the detection is given by qPCR. Moreover, the size of BMNPs is ideal not only for offering a large surface area that optimize interaction (García Rubia et al., 2018), but also for maintaining the superparamagnetism of BMNPs, which allows BMNPs to behave as non-magnetic in the absence of any magnetic field, thus preventing aggregation, and to present a large magnetic moment per particle in the presence of an external magnetic field (Valverde-Tercedor et al., 2015), thus ensuring an efficient magnetic concentration.

As a summary, the use of BMNPs allows bacteria detection to at least identical detection limit of the existing MNP-based biosensors, but without the need of using antibodies, which represents a truly simplification and step forward in the area. The experiments in this study serve as a proof of concept in the designing of easier handling and efficient biosensors and in the designing of cost- and time-effective protocols to detect bacterial contamination in liquid samples.

4. Conclusions

The results in the present paper demonstrate that BMNPs, without any further functionalization, can be efficiently used to concentrate both Gram-positive and Gram-negative microorganisms. The strategy relies in the electrostatic binding between the outer cell structures of the microorganisms and BMNPs. Following upon the application of an external magnetic field, BMNPs are able to magnetically concentrate those microorganisms. Once concentrated, the target microorganism (using *S. aureus* as a model bacterium) can be specifically detected up to bacterial loads as low as 10 CFU/mL by using qPCR. The system described here maintains (or improves) the detection limit (at least for *S. aureus*) compared to that obtained by using the Protocol ISO 6888–1:2022 and to that obtained using antibody-functionalized MNPs, thus becoming a suitable and cost-effective alternative for bacteria detection in fluid samples. The protocol for DNA extraction has been optimized to take account of the presence of BMNPs in the reaction mix and, under these conditions, no interference in qPCR reaction has been observed related to BMNPs.

Credit author statement

M.J.-C.: Methodology, Validation, Formal analysis, Investigation, Writing, Visualization. J.R.-L.: Validation, Formal analysis, Investigation, Writing. C.R.-M.: Validation, Formal analysis, Investigation, Writing. J.G.: Investigation. JM.D.: Investigation. M.M.-B.: Conceptualization, Methodology, Resources, Supervision, Project administration, Funding acquisition. A.F.-V.: Conceptualization, Methodology, Investigation, Supervision. C.J.-L.: Conceptualization, Methodology, Resources, Writing (original draft and revisions), Supervision, Project administration, Funding acquisition.

Funding sources

This work was supported by the Junta de Andalucía [P20_00208] and Ministerio de Ciencia e Innovación [PDC2021–121135-100, EQC 2019-005967-P].

Declaration of competing interest

The authors declare the following financial interests/personal relationships wh ich may be considered as potential competing interests: Concepcion Jimenez-Lopez has patent #ES2758400 licensed to UNIVERSIDAD DE GRANADA. Concepcion Jimenez-Lopez has patent #ES2758400 licensed to UNIVERSIDAD DE GRANADA.

Data availability

Data will be made available on request.

Acknowledgments

We thank the Scientific Instrumentation Center (CIC) personnel of the University of Granada for technical assistance with the TEM analyses. We thank funding through Junta de Andalucía (P20_00208) and Ministerio de Ciencia e Innovación (PDC2021–121135-100, EQC 2019-005967-P).

References

Augustine, R., Abraham, A. R., Kalarikkal, N., & Thomas, S. (2016). Monitoring and separation of food-borne pathogens using magnetic nanoparticles. *Novel Approaches of Nanotechnology in Food, 1*, 271–312. https://doi.org/10.1016/b978-0-12-804308-0.00009-1

Bhunia, A. K. (2018a). Escherichia coli. Foodborne microbial pathogens. Mechanisms and pathogenesis. In *Food science text series* (2nd ed., pp. 249–270). New York: Springer. https://doi.org/10.1007/978-1-4939-7349-1_14.

Bhunia, A. K. (2018b). Salmonella enterica. Foodborne microbial pathogens. Mechanisms and pathogenesis. In *Food science text series* (2nd ed., pp. 271–287). New York: Springer. https://doi.org/10.1007/978-1-4939-7349-1_15.

Boom, R., Sol, C., Weel, J., Lettinga, K., Gerrits, Y., van Breda, A., & Wertheim-Van Dillen, P. (2000). Detection and quantitation of human cytomegalovirus DNA in faeces. *Journal of Virological Methods, 84*(1), 1–14. https://doi.org/10.1016/s0166-0934(99)00127-5

Bülbül, G., Hayat, A., & Andreescu, S. (2015). Portable nanoparticle-based sensors for food safety assessment. *Sensors, 15*(12), 30736–30758. https://doi.org/10.3390/s151229826

Day, J. B., & Basavanna, U. (2015). Magnetic bead based immuno-detection of *Listeria monocytogenes* and *Listeria ivanovii* from infant formula and leafy green vegetables using the Bio-Plex suspension array system. *Food Microbiology, 46*, 564–572. https://doi.org/10.1016/j.fm.2014.09.020

Dragoš, A., & Kovács, Á. T. (2017). The peculiar functions of the bacterial extracellular matrix. *Trends in Microbiology, 25*(4), 257–266. https://doi.org/10.1016/j.tim.2016.12.010

Duan, N., Wu, S., Zhu, C., Ma, X., Wang, Z., Yu, Y., & Jiang, Y. (2012). Dual-color upconversion fluorescence and aptamer-functionalized magnetic nanoparticles-based bioassay for the simultaneous detection of *Salmonella Typhimurium* and *Staphylococcus aureus*. *Analytica Chimica Acta, 723*, 1–6. https://doi.org/10.1016/j.aca.2012.02.011

García Rubia, G., Peigneux, A., Jabalera, Y., Puerma, J., Oltolina, F., Elert, K., Colangelo, D., Gómez Morales, J., Prat, M., & Jimenez-Lopez, C. (2018). PH-Dependent adsorption release of doxorubicin on MamC-biomimetic magnetite nanoparticles. *Langmuir, 34*(45), 13713–13724. https://doi.org/10.1021/acs.langmuir.8b03109

Houhoula, D., Papaparaskevas, J., Zatsou, K., Nikolaras, N., Malkawi, H. I., Mingeot-Leclercq, M. P., Konteles, S., Koussisis, S., Tsakris, A., & Charvalos, E. (2017). Magnetic nanoparticle-enhanced PCR for the detection and identification of *Staphylococcus aureus* and *Salmonella enteritidis*. *New Microbiologica, 40*(3), 165–169. http://www.ncbi.nlm.nih.gov/pubmed/28513808.

Hou, J., Veeregowda, D. H., van de Belt-Gritter, B., Busscher, H. J., & van der Mei, H. C. (2017). Extracellular polymeric matrix production and relaxation under fluid shear and mechanical pressure in *Staphylococcus aureus* biofilms. *Applied and Environmental Microbiology, 84*(1). https://doi.org/10.1128/AEM.01516-17

Jabalera, Y., Oltolina, F., Peigneux, A., Sola-Leyva, A., Carrasco-Jimenez, M. P., Prat, M., Jimenez-Lopez, C., & Iglesias, G. R. (2020). Nanoformulation design including MamC-mediated biomimetic nanoparticles allows the simultaneous application of targeted drud delivery and magnetic hyperthermia. *Polymers, 12*(8), 1832–1847. https://doi.org/10.3390/polym12081832

Jabalera, Y., Sola-Leyva, A., Peigneux, A., Vurro, F., Iglesias, G. R., Vilchez-Garcia, J., Pérez-Prieto, I., Aguilar-Troyano, F. J., López-Cara, L. C., Carrasco-Jiménez, M. P., & Jimenez-Lopez, C. (2019). Biomimetic magnetic nanocarriers drive choline kinase alpha inhibitor inside cancer cells for combined chemo-hyperthermia therapy. *Pharmaceutics, 11*(8), 408–420. https://doi.org/10.3390/pharmaceutics11080408

Jacobson, K. H., Gunsolus, I. L., Kuech, T. R., Troiano, J. M., Melby, E. S., Lohse, S. E., Hu, D., Chrisler, W. B., Murphy, C. J., Orr, G., Geiger, F. M., Haynes, C. L., & Pedersen, J. A. (2015). Lipopolysaccharide density and structure govern the extent and distance of nanoparticle interaction with actual and model bacterial outer membranes. *Environmental Science and Technology, 49*, 10642–10650. https://doi.org/10.1021/acs.est.5b01841

Liébana, S., Lermo, A., Campoy, S., Cortés, M. P., Alegret, S., & Pividori, M. I. (2009). Rapid detection of *Salmonella* in milk by electrochemical magneto-immunosensing. *Biosensors and Bioelectronics, 25*, 510–513. https://doi.org/10.1016/j.bios.2009.07.022

Liébana, S., Spricigo, D. A., Cortés, M. P., Barbé, J., Llagostera, M., Alegret, S., & Pividori, M. I. (2013). Phagomagnetic separation and electrochemical magneto-genosensing of pathogenic bacteria. *Analytical Chemistry, 85*(6), 3079–3086. https://doi.org/10.1021/ac3024944

Li, Y., Wang, Z., Sun, L., Liu, L., Xu, C., & Kuang, H. (2019). Nanoparticle-based sensors for food contaminants. *TrAC, Trends in Analytical Chemistry, 113*, 74–83. https://doi.org/10.1016/j.trac.2019.01.012

Meysman, P., Sánchez-Rodríguez, A., Fu, Q., Marchal, K., & Engelen, K. (2013). Expression divergence between *Escherichia coli* and *Salmonella enterica* serovar Typhimurium reflects their lifestyles. *Molecular Biology and Evolution, 30*(6), 1302–1314. https://doi.org/10.1093/molbev/mst029

Naderlou, E., Salouti, M., Amini, B., Amini, A., Narmani, A., Jalilvand, A., Shahbazi, R., & Zabihian, S. (2020). Enhanced sensitivity and efficiency of detection of *Staphylococcus aureus* based on modified magnetic nanoparticles by photometric systems. *Artificial Cells, Nanomedicine, and Biotechnology, 48*(1), 810–817. https://doi.org/10.1080/21691401.2020.174863

Peigneux, A., Oltolina, F., Colangelo, D., Iglesias, G. R., Delgado, A. V., Prat, M., & Jimenez-Lopez, C. (2019). Functionalized biomimetic magnetic nanoparticles as effective nanocarriers for targeted chemotherapy. *Particle & Particle Systems Characterization, 36*(6), Article 1900057. https://doi.org/10.1002/ppsc.201900057

Perez-Gonzalez, T., Rodriguez-Navarro, A., & Jimenez-Lopez, C. (2011). Inorganic magnetite precipitation at 25°C: A low-cost inorganic coprecipitation method. *Journal of Superconductivity and Novel Magnetism, 24*(1–2), 549–557. https://doi.org/10.1007/s10948-010-0999-y

Prozorov, T., Bazylinski, D. A., Mallapragada, S. K., & Prozorov, R. (2013). Novel magnetic nanomaterials inspired by magnetotactic bacteria: Topical review. *Materials Science and Engineering: R: Reports, 74*(5), 133–172. https://doi.org/10.1016/J.MSER.2013.04.002

Samuel, G., & Reeves, P. (2003). Biosynthesis of O-antigens: Genes and pathways involved in nucleotide sugar precursor synthesis and O-antigen assembly. *Carbohydrate Research, 338*, 2503–2519. https://doi.org/10.1016/j.carres.2003.07.009

Stenutz, R., Weintraub, A., & Widmalm, G. (2006). The structures of *Escherichia coli* O-polysaccharide antigens. *FEMS Microbiology Reviews, 30*(3), 382–403. https://doi.org/10.1111/j.1574-6976.2006.00016.x

Sung, Y. J., Suk, H.-J., Sung, H. Y., Li, T., Poo, H., & Kim, M.-G. (2013). Novel antibody/gold nanoparticle/magnetic nanoparticle nanocomposites for immunomagnetic separation and rapid colorimetric detection of *Staphylococcus aureus* in milk. *Biosensors and Bioelectronics, 43*, 432–439. https://doi.org/10.1016/j.bios.2012.12.052

Su, X., Wang, M., Ouyang, H., Yang, S., Wang, W., He, Y., & Fu, Z. (2017). Bioluminescent detection of the total amount of viable Gram-positive bacteria isolated by vancomycin-functionalized magnetic particles. *Sensors and Actuators B: Chemical, 241*, 255–261. https://doi.org/10.1016/j.snb.2016.10.042

Ubago-Rodríguez, A., Casares Atienza, S., Fernández-Vivas, A., Peigneux, A., Jabalera, Y., De La Cuesta-Rivero, M., Jimenez-Lopez, C., & Azuaga Fortes, A. I. (2019). Structure-function of MamC loop and its effect on the in vitro precipitation of biomimetic magnetite nanoparticles. *Crystal Growth & Design, 19*(5), 2927–2935. https://doi.org/10.1021/acs.cgd.9b00150

Valverde-Tercedor, C., Montalbán-López, M., Perez-Gonzalez, T., Sanchez-Quesada, M. S., Prozorov, T., Pineda-Molina, E., Fernandez-Vivas, M. A., Rodriguez-Navarro, A. B., Trubitsyn, D., Bazylinski, D. A., & Jimenez-Lopez, C. (2015). Size control of in vitro synthesized magnetite crystals by the MamC protein of *Magnetococcus marinus* strain MC-1. *Applied Microbiology and Biotechnology, 99*(12), 5109–5121. https://doi.org/10.1007/s00253-014-6326-y

Wang, Y., Ravindranath, S., & Irudayaraj, J. (2011). Separation and detection of multiple pathogens in a food matrix by magnetic SERS nanoprobes. *Analytical and Bioanalytical Chemistry, 399*, 1271–1278. https://doi.org/10.1007/s00216-010-4453-6

Yuan, J., Tao, Z., Yu, Y., Ma, X., Xia, Y., Wang, L., & Wang, Z. (2014). A visual detection method for *Salmonella Typhimurium* based on aptamer recognition and nanogold labeling. *Food Control, 37*, 188–192. https://doi.org/10.1016/j.foodcont.2013.09.046

Yu, H., Raymonda, J. W., McMahon, T. M., & Campagnari, A. A. (2000). Detection of biological threat agents by immunomagnetic microsphere-based solid phase fluorogenic- and electro-chemiluminescence. *Biosensors and Bioelectronics, 14*(10), 829–840. https://doi.org/10.1016/S0956-5663(99)00068-8

Glossary

MNPs: magnetic nanoparticles
BMNPs: biomimetic magnetic nanoparticles
FPLC: Fast Protein Liquid Chromatography
XRD: powder X-ray diffraction
TEM: transmission electron microscopy
EELS: electron energy loss spectroscopy
iep: isoelectric point